ARTICLES
PUBLISHED ONLINE: 5 FEBRUARY 2012 | DOI: 10.1038/NPHOTON.2011.350
nature photonics

Comb-based radiofrequency photonic filters with rapid tunability and high selectivity

V. R. Supradeepa†‡, Christopher M. Long†‡, Rui Wu‡, Fahmida Ferdous, Ehsan Hamidi†, Daniel E. Leaird and Andrew M. Weiner*

Photonic technologies have received considerable attention regarding the enhancement of radiofrequency electrical systems, including high-frequency analogue signal transmission, control of phased arrays, analog-to-digital conversion and signal processing. Although the potential of radiofrequency photonics for the implementation of tunable electrical filters over broad radiofrequency bandwidths has been much discussed, the realization of programmable filters with highly selective filter lineshapes and rapid reconfigurability has faced significant challenges. A new approach for radiofrequency photonic filters based on frequency combs offers a potential route to simultaneous high stopband attenuation, fast tunability and bandwidth reconfiguration. In one configuration, tuning of the radiofrequency passband frequency is demonstrated with unprecedented (∼40 ns) speed by controlling the optical delay between combs. In a second, fixed filter configuration, cascaded four-wave mixing simultaneously broadens and smoothes the comb spectra, resulting in Gaussian radiofrequency filter lineshapes exhibiting an extremely high (>60 dB) main lobe to sidelobe suppression ratio and (>70 dB) stopband attenuation.

Optical frequency combs, generated by means of self-referenced and stabilized mode-locked lasers, have enabled revolutionary progress in precision optical frequency synthesis and metrology[1–4]. Optical combs are also of tremendous interest in other applications[5], including multiwavelength coherent lightwave communications[6–8], optical arbitrary waveform generation[9–11], the generation of low-phase-noise[12] or agile ultrabroadband microwaves[13], and signal processing[6,14]. For these purposes, in which higher pulse repetition rates are desired and only moderate frequency stability is required, comb sources based on strong electro-optic modulation of a continuous-wave (c.w.) laser have attracted a substantial amount of attention[15,16]. Here, we report significant advances in radiofrequency (RF) photonic filters enabled by the ability to rapidly tune the timing of the comb and shape its power spectrum.

In general, RF photonics has received considerable attention due to the low-loss properties of optical fibres, which can be harnessed for the transmission of RF signals (in optical form) over distances and bandwidths that would not be possible with RF cables, as well as for immunity to electromagnetic interference and reduced weight[17–19]. For signal-processing applications, the high carrier frequency is a fundamental consideration empowering photonics approaches; for example, even a 20 GHz RF bandwidth constitutes only 0.01% of the optical central frequency. Although rapidly reconfigurable RF filters could have significant implications for concepts such as cognitive radio, in which the radio may tune adaptively to use free regions of the RF spectrum[20,21], the tuning of RF filters over a large fractional bandwidth has traditionally been difficult. However, bandwidths that are large and challenging to work with in the RF domain are relatively small when translated into the optical regime and may be much easier to handle[22,23]. The introduction of microelectromechanical systems (MEMS) variable capacitor approaches has led to recent advances in tunable RF filters[24–26]. The fundamental tuning speed of RF MEMS devices is characterized in ref. 24 as being limited to ∼1–300 μs. Filters based on solid-state diodes have fundamentally higher tuning speeds but suffer from increased nonlinearity, loss and power consumption[24]. In either technology, challenges in controlling the coupled response of multiple resonances to maintain high filter selectivity practically constrain tuning to speeds much slower than the fundamental limits. In photonics, one approach seeks to achieve RF filtering by transmitting RF modulation sidebands of an optical carrier through an optical filter. In one example, apparently based on a cascade of five coupled optical microresonators, a fifth-order filter with 70 dB stopband suppression[27] has been reported. However, as in filters implemented directly in the RF domain, tuning is complex, because changes to the individual resonators must be synchronized to maintain the desired multipole filter function[28]. Rapid tuning of the RF filter response by tuning the laser frequency relative to the optical filter has been proposed[28]. However, rapidly (for example, submicrosecond) controllable tuning of a c.w. laser over a range of a few gigahertz is itself a difficult challenge, and to the best of our knowledge the use of this technique to realize rapid RF filter tuning has not been demonstrated.

A different and more heavily studied approach for RF photonic filters follows a tapped delay line architecture[17–19]. In contrast to coupled resonator approaches, tapped delay lines yield finite impulse response (FIR) filters characterized by the zeroes of the response function[29]. Such FIR filters are commonly considered for digital filter design and provide substantial flexibility for engineering both amplitude and phase response[30,31]. Broadband light sources such as mode-locked lasers[32,33] or c.w. incoherent light[34] have recently been exploited, in conjunction with dispersive propagation, to scale RF photonic tapped delay line filter implementations to a large number of RF taps with a single physical light source and a

School of Electrical and Computer Engineering, Purdue University, West Lafayette, Indiana, USA; †Present address: OFS Laboratories, Somerset, New Jersey, USA (V.R.S.); EPFL, Lausanne, Switzerland (C.M.L.); Wellman Center for Photomedicine, Massachusetts General Hospital, Boston, Massachusetts, USA (E.H.); ‡These authors contributed equally to this work. *e-mail: amw@ecn.purdue.edu

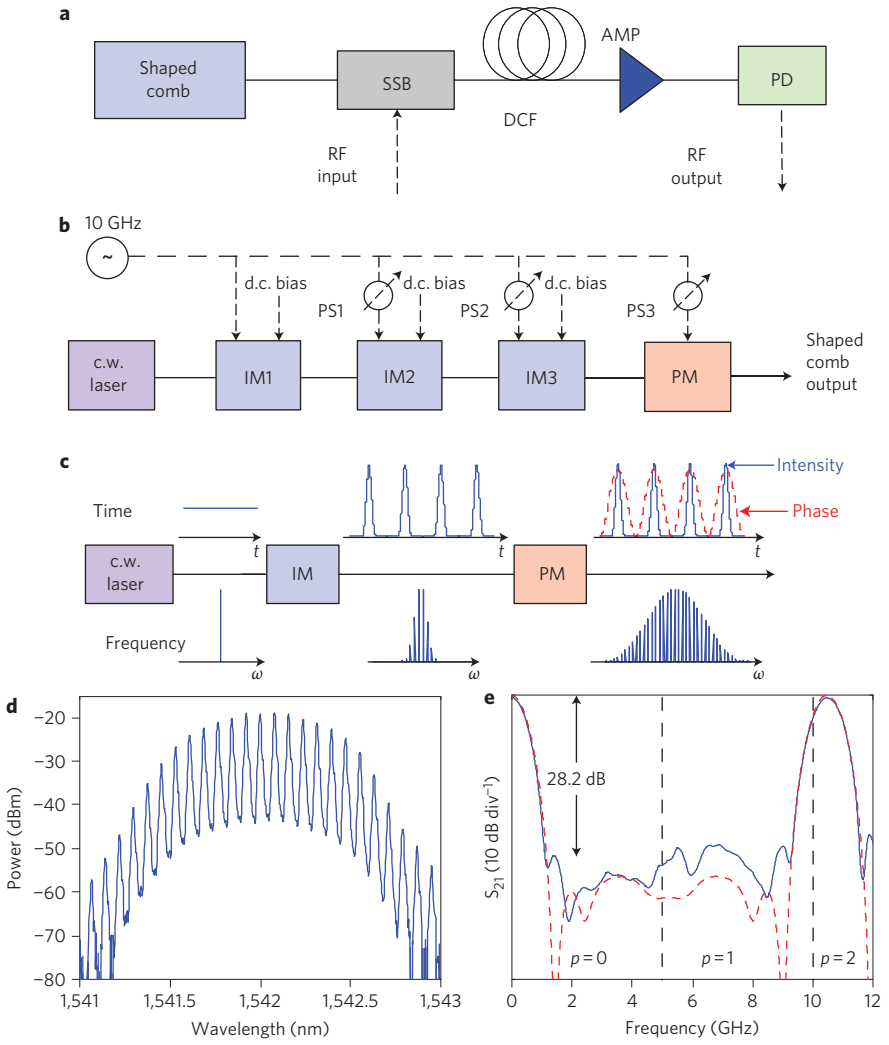

Figure 1 | Representative operation of an optical frequency comb-based multi-tap RF photonic filter. a, Schematic of a multi-tap microwave photonic filter using an optical frequency comb. SSB, single-sideband modulation; DCF, dispersion-compensating fibre; AMP, fibre amplifier; PD, photodetector, **b**,**c**, Experimental scheme (**b**) and pictorial representation (**c**) of direct quasi-Gaussian frequency comb generation. c.w., continuous-wave laser; IM, intensity modulator; PM, phase modulator; PS, microwave phase shifter. **d**, Optical spectrum of generated frequency comb. **e**, Measured (blue) and simulated (red) RF filter response using this comb. The vertical dashed lines depict individual Nyquist zones (for explanation see Methods).

single delay element. Recently, the use of a recirculating frequency shifter as a tapped delay line yielded filters with passbands centred in the 100–200 MHz range, a free spectral range (FSR) of ~35 MHz, main-to-sidelobe suppression ratio (MSSR) of 52 dB and a stopband attenuation of >70 dB (ref. 35). However, tuning was not demonstrated. Finally, in ref. 14 we demonstrated an approach for the photonic implementation of RF electrical filters based on electro-optically generated frequency combs apodized using a programmable pulse shaper[36]. These filters have central frequencies and FSRs in the gigahertz range and bandwidths of hundreds of megahertz, appropriate for channelization of RF spectra at a resolution matched to electronic analog-to-digital converter technology. However, the full potential of optical frequency combs has not been explored.

Here, we introduce several new concepts in comb-based RF photonics that bring special advantages for filter shape and tunability. First, careful tailoring of the comb spectral profile may be accomplished through the nonlinear interaction of a pair of synchronized, frequency-offset combs directly as part of the generation process and without the need for a pulse shaper. The extreme smoothness of the resulting spectrum leads to tapped delay line filters with greatly enhanced MSSR. Second, the relative delay between a synchronized pair of combs can be switched in tens of nanoseconds, which translates into similarly rapid switching of the RF passband. An important point in our approach is that the filter lineshape is in principle independent of filter tuning, which substantially eases control complexity. The possibility of bandwidth reconfigurability is also demonstrated. Comb-based RF photonic filter configurations offer the potential to provide, simultaneously, a high number of taps, fast tunability, bandwidth reconfiguration and high stopband attenuation, a combination difficult to achieve with other known approaches.

Results

Figure 1a presents a schematic of an optical frequency comb-based RF photonic filter. A comb of optical frequencies spaced by $\Delta f \approx 10$ GHz was generated by periodic intensity and phase modulation of a c.w. laser[15,16], then passed through a single-sideband modulator driven by the RF signal that we wished to filter. This placed an identical sideband onto each of the optical comb lines. The signal then propagated through a dispersive fibre and was converted back to the RF domain using a photodetector. In this arrangement, comb lines arrive at the photodetector with different delays and hence function as independent taps in a tapped delay line

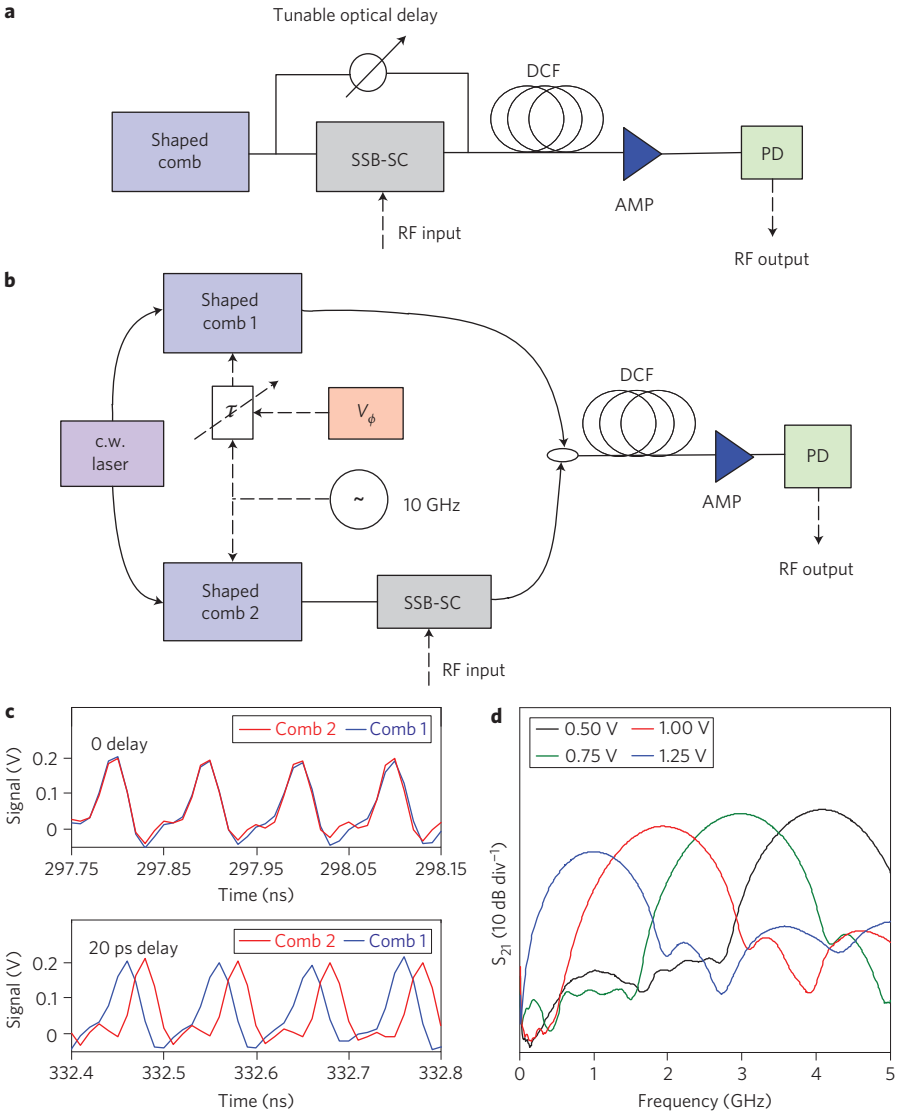

Figure 2 | Achieving rapid electronic frequency tunability of the RF filter using a dual-comb approach. a, Scheme depicting the use of optical delay between combs to achieve filter tunability. SSB-SC, single-sideband modulation with suppressed carrier. **b**, Method to achieve rapid tunability using a dual-comb scheme. **c**, Experimental results showing the programmable rapid delay tuning between the two combs by applying a rapid step to the RF phase shifter. **d**, Tuning the centre frequency of the RF filter by changing the voltage to the phase shifter (quasi-static case).

filter architecture. The RF impulse response $h(t)$ and frequency response $H(\omega)$ can be written as[14]

$$h(t) \propto \sum_{n=0}^{N-1} |e_n|^2 \delta(t - nT) \quad \text{and} \quad H(\omega) \propto \sum_{n=0}^{N-1} |e_n|^2 e^{-jn\omega T} \qquad (1)$$

where e_n is the electric field amplitude of the nth line of the comb and $T = 2\pi\Delta f\psi_2$ is the differential delay between comb lines, determined by the group delay dispersion ψ_2 and the frequency spacing between comb lines, Δf. From equation (1), the RF filter has a periodic frequency response with an FSR of T^{-1} and passband shape governed by the Fourier transform of the optical comb spectrum. By properly apodizing (or shaping) the comb spectrum, filters with high stopband attenuation and user-defined passband functions may be achieved. Here, we focus on filters with passbands that are approximately Gaussian, a shape that provides fast roll-off in both frequency and time domains. Previously, we used a high-resolution pulse shaper[9,36] to shape the comb spectrum, resulting in a stopband attenuation as low as ~35 dB, limited by the 0.37 dB ripple in the apodized spectrum (see Supplementary Information)[14]. Here, we realize substantially improved passband shapes by introducing new methods for shaping the comb directly in the generation process.

Figure 1b presents our set-up for the direct generation of an approximately Gaussian comb spectrum (the principle is shown in Fig. 1c). Three cascaded lithium niobate intensity modulators generate a train of 10 GHz pulses that are approximately Gaussian in time, to which we then apply a strong sinusoidal phase modulation. For pulsed signals centred at extrema of the sinusoid, the temporal phase is approximately quadratic, which results in time-to-frequency mapping, with the temporal intensity of the waveform mapped onto its power spectrum[37,38]. This time-to-frequency mapping enables the direct generation of an approximately Gaussian frequency comb. Figure 1d shows the spectrum generated using this scheme, and Fig. 1e the frequency response of the RF photonic filter, measured using a vector network analyser (VNA) and overlaid with a simulation based on equation (1) and the measured comb spectrum. As expected, we see two Gaussian-like passbands separated by the filter FSR. Fibre dispersion produces a tap delay of $T = 96$ ps and a corresponding FSR of 10.4 GHz. The

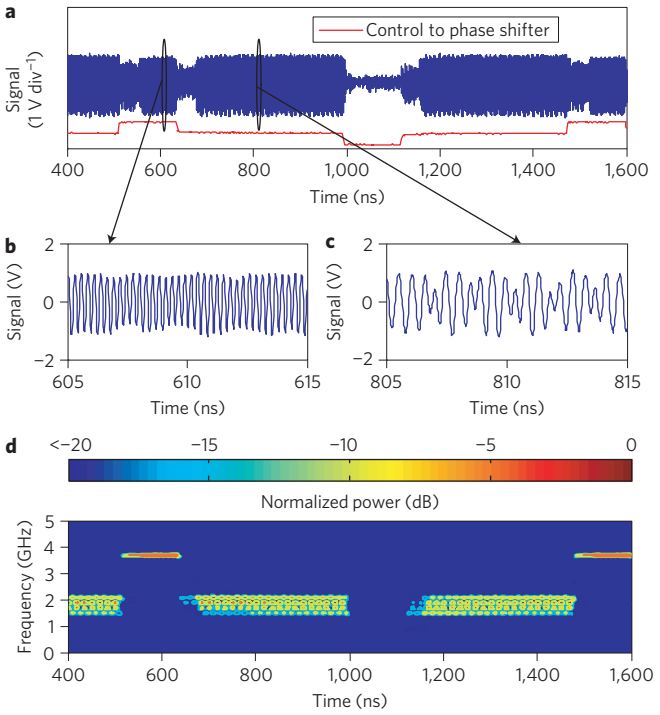

Figure 3 | Rapid frequency tunability of the RF filter. a, Measured oscilloscope signal demonstrating rapid switching between different frequency bands. Also shown is the control signal input to the phase shifter. **b**, Close-up of a first waveform part of the signal (a 3.7 GHz RF tone). **c**, Close-up of a second waveform section (a 1.8 GHz RF tone undergoing binary phase-shift keying at 600 Mb s^{-1}). **d**, Spectrogram representation of the filtered signal, highlighting rapid switching between different frequency bands.

passband centred at 10.4 GHz has a 3 dB bandwidth of 750 MHz, with a stopband attenuation of >28 dB. Overall, the measured filter function is close to the simulated response based on the comb spectrum, which confirms the predicted Fourier-transform relationship.

Rapidly frequency-tunable RF photonic filters

Although the passband frequency may be tuned in the scheme of Fig. 1 by changing the amount of dispersion, this is inconvenient and not rapidly adjustable. Recently, we proposed a new approach to achieve filter tuning with fixed dispersion[14], as shown schematically in Fig. 2a. This method makes use of an interferometric configuration in which one sample of the comb is single-sideband-modulated with the carrier suppressed, and a second sample of the comb remains unmodulated but experiences a tunable optical delay. The frequency response of the RF filter, obtained after the two samples of the comb are combined, sent down a dispersive line, and detected, can be written as[14]:

$$H(\omega) \propto \sum_{n=0}^{N-1} e_{1n} e_{2n}^{*} e^{-jnT(\omega-\tau/\psi_2)} \qquad (2)$$

where e_{1n} and e_{2n} are the complex electric field amplitudes of the nth comb line in the two arms of the interferometer and τ is the relative delay between the two optical paths. If e_{1n} and e_{2n} are from the same comb, their phases will cancel, again leading to tap amplitudes given by $|e_n|^2$, that is, by the comb spectrum. Equation (2) shows that the centre frequency of the filter can be controlled by the relative delay. This was demonstrated for the first time in ref. 14, which used a mechanical delay line to achieve quasi-static tuning.

In this Article, we introduce a new scheme that takes advantage of dual electro-optically generated frequency combs to achieve a radically enhanced tuning speed, as shown in Fig. 2b. A single c.w. laser is split and directed into two nominally identical comb generators, each following the approach of Fig. 1b. As above, one of the combs is single-sideband-modulated (but now with a suppressed carrier), while the other remains unmodulated but is provided with controllable delay. A key observation is that because the two comb generators are driven at the same RF frequency, the relative delay of the generated optical trains is governed by the relative phase shift of the respective RF drive signals. Analogue RF phase shifters are available that can vary the phase over a 2π range with >50 MHz modulation bandwidth. By using such a phase shifter, the delay of the generated comb can be electronically tuned over a full comb period in tens of nanoseconds. Figure 2c demonstrates rapid tuning of the optical delay between combs. The experiment is set up so that the two comb signals are initially overlapped in time (top panel). A step input to the control port of the RF phase shifter induces a change in the relative delay. As seen in the bottom panel, one of the optical pulse trains is shifted in this example by 20 ps (corresponding to ~20% of the comb repetition period) in <30 ns. This permits tuning of the RF filter response within a comparable time span, substantially faster than conventional RF tunable filter technologies with potential for high selectivity.

Figure 2d shows quasi-static tuning of the filter. By changing the control voltage into the phase shifter by only 0.75 V, the filter passband is shifted 3 GHz. The varying gain is attributed to the periodic optical filter used for carrier suppression in the single-sideband modulation with suppressed carrier (SSB-SC) block, which also attenuates RF sideband signals that are close to the carrier. Gain variation could be substantially reduced by using a periodic optical notch filter with sharper edges, such as an etalon in reflection mode. Important points are (i) that the passband shape, bandwidth and stopband attenuation (~30 dB) are similar to the filter response of Fig. 1 and (ii) that these quantities remain largely unchanged when the filter is tuned. In agreement with the predictions of equation (2), the filter frequency may be tuned independently of the passband shape; this greatly simplifies high-speed tuning of such filters. This property has been demonstrated previously using microwave delay-line filters with complex coefficients[39,40], but implementation complexity has limited the number of taps, and fast tuning was not reported.

The novel blend of electronic technologies and optics in our set-up enables tuning at high speed and over a broad bandwidth, simultaneously. To view the response of such rapidly time-varying filters, a time-domain measurement technique (as opposed to pervasive frequency-domain methods based on network analysers) is absolutely required. An RF test waveform in which a 3.7 GHz tone and a 1.8 GHz carrier subject to a 600 Mb s^{-1} binary phase-shift keying modulation are superimposed and input into the SSB-SC modulator, and a high-speed control signal is connected to the control port of the phase shifter. Figure 3a shows a high-level view of the RF signal at the output of the photodiode and of the control signal to the RF phase shifter (shifted to account for the filter latency). The control signal comprises three different voltage levels that tune the filter to three different central frequencies. Zoomed-in sections of oscilloscope traces of the filter output, corresponding to high- and mid-level control voltages for which 3.7 and 1.8 GHz input signals are individually selected, are shown in Fig. 3b and c, respectively. The low control voltage tunes the filter to a frequency band not present on the input signal, and the filter output goes low. Figure 3d shows a spectrogram of the data set, which provides an intuitive visual

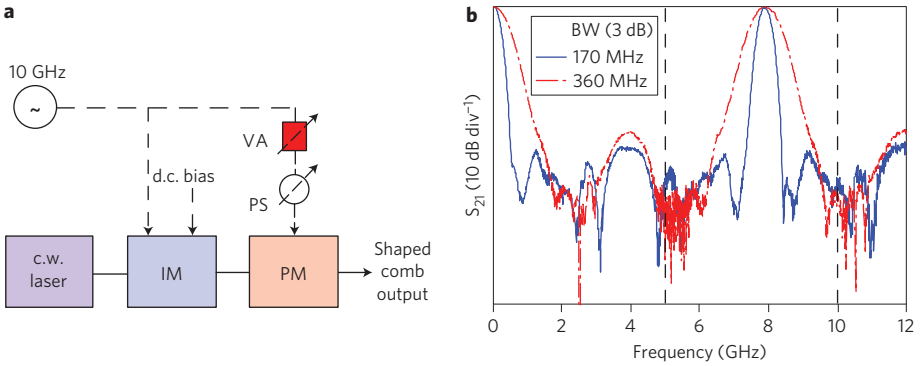

Figure 4 | Demonstration of the bandwidth tunability of the RF filter. a, Scheme for modifying the bandwidth of the generated optical comb. VA, variable RF attenuator. **b**, RF filter passbands obtained with different drive voltages applied to the phase modulator of **a**. Bandwidth tuning by a factor of two is demonstrated. BW, bandwidth.

representation of the time–frequency character of the filtered signal. The different frequency components superimposed at the input are now separated in time, and the presence of modulation on the 1.8 GHz signal is clearly evident as increased bandwidth. Examination of the rapid transitions between output frequency components reveals that the filter is able to switch within 40 ns, limited by the response time of the RF phase shifter. Such rapid filter tuning is unprecedented in RF photonics and is substantially beyond the demonstrated capabilities of any known high-selectivity filter technology.

Bandwidth reconfigurability

In addition to tuning, in which the filter passband is shifted rigidly in frequency, reconfiguration of the passband shape is also of interest. Here, we demonstrate reconfiguration of the filter bandwidth. According to equation (1), the RF bandwidth varies inversely with the bandwidth of the optical comb, which in turn is proportional to the RF drive signal to the phase modulator. By placing a variable attenuator before the phase modulator, as shown in Fig. 4a, the generated optical bandwidth may be varied. Figure 4b shows measured RF transfer functions in a fixed filter configuration. By reducing the drive voltage to the phase modulator by a factor of approximately two, the optical bandwidth is decreased by a similar factor, resulting in an increase in RF bandwidth from 170 MHz to 360 MHz. The filter shapes remain similar, in each case with >30 dB MSSR. These proof-of-concept results make use of a manually variable attenuator, allowing quasi-static reconfiguration; however, by upgrading to electronically controllable RF attenuators, a bandwidth reconfiguration within tens of nanoseconds is anticipated. We also note that because this bandwidth reconfiguration scheme is fundamentally independent of the frequency tunability demonstrated earlier, in the future it should be possible to achieve simultaneous, independent and rapid control of both passband frequency and bandwidth. This could be done by provisioning both of the 'shaped combs' of Fig. 2b with electronically controllable RF attenuators so that their optical bandwidths can be modulated in an identical fashion.

Improving passband shape

We now focus on a final important attribute for filter applications, namely selectivity, manifested through a high MSSR and stopband attenuation. The key to high selectivity in our scheme is to achieve an extremely smooth and specifically shaped comb spectrum with minimal line-to-line variations. Direct electro-optic generation of an approximately Gaussian comb, described above, is a first step, but substantial improvement in spectral shaping is still required. Here, we introduce a dual-laser-driven comb generator plus nonlinear fibre-optics approach that simultaneously broadens and smoothes the comb spectrum to achieve selective filters with greatly enhanced MSSR and stopband attenuation. High-efficiency frequency conversion through four-wave mixing (FWM) has been used previously for a variety of tasks in optical communications[41,42]. Here, we utilize cascaded FWM as a phase modulation amplifier and spectral smoother.

Figure 5a shows the experimental set-up for the comb generator. As in Fig. 1b, electro–optic intensity and phase modulators produce a quasi-Gaussian spectrum on a c.w. laser centred at 1,542 nm. A second c.w. laser (1,532 nm) is combined without intensity modulation and passes through the same phase modulator. For reasons that will become clear, one comb is delayed with respect to the other by one-half of the modulation period (50 ps at 10 GHz). This is followed by an amplifier and zero-dispersion, low-dispersion-slope highly nonlinear fiber (HNLF). Cascaded FWM in the HNLF leads to amplification of the phase modulation and substantial spectral broadening and smoothing. Figure 5b shows a schematic of the comb generation process. The initial two combs have narrow bandwidth and poor spectral quality.

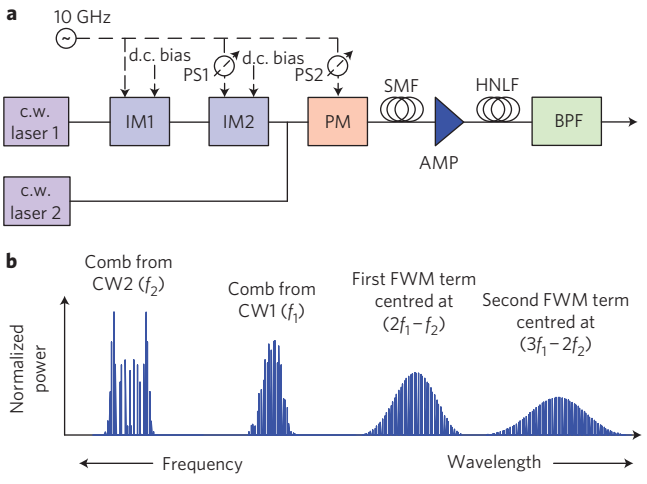

Figure 5 | Direct, high-accuracy generation of Gaussian apodized broadband combs. a, Experimental scheme to directly generate broadband, apodized combs using cascaded FWM in a HNLF. The electro-optic modulator portion of the comb generator is similar to Fig. 1b, but simplified by reducing the number of IMs. SMF, single-mode fibre; HNLF, highly nonlinear fibre; BPF, bandpass filter. **b**, Depiction of the cascaded FWM process. Successive terms scale in bandwidth and correspond increasingly accurately to a smooth Gaussian apodization.

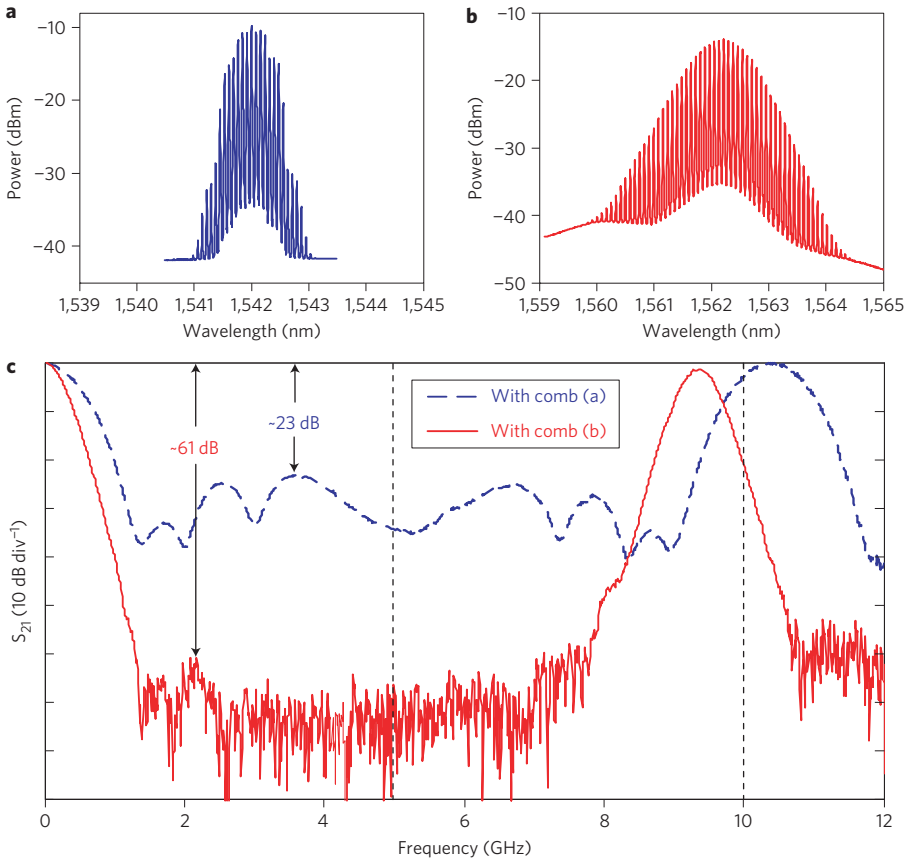

Figure 6 | Achieving high stop-band attenuation RF filters. a, Spectrum from laser CW1 measured directly after the modulators. **b**, Measured spectrum of the second-order cascaded FWM term used in our experiment. **c**, Measured RF filter transfer function using the second-order FWM term (**b**), demonstrating an extremely high main lobe to sidelobe suppression ratio (61 dB) and stop-band attenuation (>70 dB). Also shown is the measured transfer function using only the comb after the modulators (**a**).

However, for successive FWM terms the bandwidth increases and the spectral shape becomes more Gaussian.

To understand this process more quantitatively, let $a_1 = |a_1(t)|\exp(j\varphi(t))$ be the complex amplitude of laser 1 (centred at f_1), which undergoes intensity and phase modulation. The intensity envelope $|a_1(t)|^2$ is shaped to look roughly Gaussian, and the temporal phase $\varphi(t)$ is sinusoidal. Laser 2 (centred at f_2) is only phase modulated, and its complex amplitude can be written as $a_2 = \exp(j\varphi(t))$. After transmitting through a length of single-mode fibre (SMF), which delays laser 2 by half a modulation period with respect to laser 1, the complex amplitude of laser 2 can be written as $a_2 = \exp(-j\varphi(t))$. In the HNLF, these waveforms mix to give a cascade of FWM terms. In the limit of negligible dispersion, the first FWM term centred at $(2f_1 - f_2)$ will be primarily composed of

$$a_1^{\,2}a_2^{\,*} = |a_1(t)|^2 \exp(j3\varphi(t)) \tag{3}$$

Similarly, the second-order FWM will expressed as

$$a_1^{\,3}a_2^{\,2*} = |a_1(t)|^3 \exp(j5\varphi(t)) \tag{4}$$

Equations (3) and (4) correspond to scaling of the bandwidth by factors of three and five, respectively. Furthermore, as the temporal intensity profile becomes increasingly localized as it is raised to progressively higher powers, the temporal phase is increasingly well approximated as quadratic. This results in higher-fidelity time-to-frequency mapping and increasingly smooth combs.

Figure 6a,b shows the comb spectrum of laser 1 immediately after the modulators and of the second-order FWM term, respectively. Both bandwidth enhancement and spectral smoothing are clearly seen. Figure 6c shows the corresponding filter transfer functions. The measured filter functions have different FSRs due to the 20 nm redshift of the second-order FWM signal and the dispersion slope of the dispersion-compensating fibre (DCF) module. The filter response (blue dashed line) for the comb shown in Fig. 6a has a peak at baseband with a 3 dB bandwidth of 350 MHz, whereas at 10.4 GHz there is a passband with 800 MHz, 3 dB bandwidth. The filter response (red solid line) for the comb shown in Fig. 6b has a peak at baseband with a 3 dB bandwidth of 210 MHz, while at 9.38 GHz (corresponding to 107.5 ps tap delay) there is a passband with 440 MHz, 3 dB bandwidth. The roughly twofold reduction in passband width is attributed to the increased comb bandwidth. Most importantly, the MSSR and stopband suppression are increased to 61 dB and >70 dB, respectively, the latter limited by the VNA noise floor. Simulations (see Supplementary Information) suggest that to reach these levels of performance, random variations of the comb spectrum must have a standard deviation below ~0.2% (9×10^{-3} dB). Such variations are ~40 times smaller than previous results, in which apodization of a comb was performed using a pulse shaper[14], leading to improvements in MSSR and stopband attenuation of >25 dB. The level of sidelobe suppression and stopband attenuation demonstrated here is extremely rare in RF photonics; to our knowledge comparable levels are reported only in refs 27 and 35. Furthermore, by incorporating our new nonlinear optical spectral smoothing approach into the tunable comb-based RF filter discussed earlier, in the future it should be possible to

achieve high-dynamic-range lineshapes together with extremely rapid tunability, a combination very difficult to achieve using other approaches.

Discussion

An important point to note regarding our approach is that filter lineshape is in principle independent of filter tuning, so, once sufficiently selective filter shapes are achieved, tuning should be possible with little additional control complexity. Rapid control of the RF bandwidth should also be possible. These operations could support a novel spectral zoom functionality, in which the RF spectrum is first scanned with a relatively coarse filter, which then zooms in to selected regions of interesting RF activity. Similar advantages should also extend to other types of filter response functions, including pulse compression filters. This is in marked contrast to conventional realizations of highly selective RF filters, which involve the coupled response of multiple resonances. Because of this coupling, tuning while maintaining highly selective lineshapes is difficult, and control is challenging.

Our approach is based fundamentally on the concept of an RF photonic link, modified to realize filtering action, specifically demonstrating a route to simultaneous tuning, bandwidth control, and high MSSR and stopband attenuation. As a result of inefficient RF $\rightarrow$ optical $\rightarrow$ RF transduction, achieving a good RF link performance has traditionally been challenging. Our filters are subject to the same challenges and currently exhibit $\sim$40 dB RF insertion loss at 0.5 mA photodetector current, which is not good enough for practical applications. However, using special low V_π modulators and high-current-handling detectors, dramatically improved RF photonic links have been realized in the last several years[43,44], with a RF gain $>$10 dB and noise figure of $<$6 dB demonstrated at frequencies beyond 10 GHz (ref. 43). Analysis shows that the RF gain and noise figure of a short optical link based on modulation of a frequency comb obey the same expressions as links based on a single laser[45]. Furthermore, for fibre remoting applications involving long RF photonic transmission links, the use of comb sources has recently been shown to suppress Brillouin scattering, enabling higher optical power and improved RF link performance[46]. Therefore, with appropriate investment in state-of-the-art components, in the future it should be possible to realize comb-based RF photonic filters both with the novel tuning, reconfiguration, and filter selectivity properties introduced here and with significantly improved link performance.

In addition to direct electro-optic comb generation, our comb-based RF photonic filtering scheme may also be implemented with other comb sources synchronizable to a RF drive. These include recirculating frequency shifters as in ref. 35, scaled to higher comb spacing by using a single-sideband electro-optic modulator in an amplifying loop[47], as well as integrated Fourier-domain mode-locked lasers as proposed in ref. 48. Such sources may offer an increase in comb power, which would facilitate improvements in RF gain. Finally, sampling considerations limit the frequency span of our RF photonic filter that is free from Nyquist spurs to half of our 10 GHz comb repetition frequency[14] (see Methods). By using higher-frequency optical modulators (already developed for optical communications), we can anticipate increasing comb spacings to at least 40 GHz, boosting the spur-free range of our comb-based RF photonic filters by at least a factor of four.

In summary, we have demonstrated several new principles for RF photonic filters based on electro-optically generated frequency combs. A novel nonlinear optics approach enhances both the bandwidth and shape of the combs, leading to $>$60 dB MSSR and $>$70 dB RF stopband attenuation in a fixed filter geometry. Switching of optical delay under electronic control leads to extremely rapid ($\sim$40 ns) tuning of the filter response, while proof-of-concept experiments point the way to potentially rapid bandwidth reconfigurability.

Methods

Filter components. Our RF photonic filters were constructed using a single-sideband modulator, a 5.1-km-long DCF with a specified dispersion of $-1{,}259.54$ ps nm^{-1}, and a 20 GHz bandwidth photodetector. For the bandwidth reconfiguration experiments of Fig. 4, additional fibre was used that increased the overall dispersion by 31.7%, which reduced the FSR of the filter from 10.4 GHz to 7.9 GHz. RF connections were made with conventional coaxial cables with specified 18 GHz bandwidth. Single-sideband modulation was achieved using a dual-drive lithium niobate Mach–Zehnder modulator, which may be viewed as an interferometer with independent phase modulators in its two arms[49]. By driving the phase modulators with 90° RF phase shift and biasing the interferometer at 90° optical phase shift, one of the modulation sidebands could be cancelled, leaving just a single sideband on each comb line. Our dual-drive modulator had a half-wave voltage of 4.5 V at 1 kHz and a 3 dB bandwidth of 12.2 GHz. The phase shift between the RF drive signals was provided by a 90° hybrid splitter with a bandwidth of 1–12.4 GHz and a maximum phase imbalance of 7°. For the tunable filter experiments, we also suppressed the carriers by using a periodic optical filter with nulls positioned at the comb frequencies. This was realized using a micro-optic interferometer with $\sim$100 ps delay imbalance, implemented as a commercial differential phase-shift keying (DPSK) demodulator.

Measurement techniques. Comb spectra were measured using an optical spectrum analyser (OSA) with a resolution of 0.01 nm. RF filter frequency response measurements were performed using a VNA, usually set for 10 Hz resolution bandwidth. Before plotting, frequency responses were normalized by subtracting out the response measured in a fixed filter configuration but without the dispersive fibre. This took out RF frequency dependencies due to cable loss and high-frequency component roll-off, thereby focusing on the RF response intrinsically related to our photonic processing scheme[14].

Because of the periodic nature of discrete-time filters, unwanted higher-order mixing terms may also be generated by this filter. For instance, an optical sideband may mix with a neighbouring comb line to produce a signal that is located in a higher frequency band. As discussed in detail elsewhere[14], a variety of tones at frequencies $m\Delta f$ and $m\Delta f \pm f_{\mathrm{RF}}$ may be present at the output, where f_{RF} is the frequency of a single RF input tone, Δf is the comb spacing and m is an integer. To avoid aliasing related to such effects, sampling theory restricts the operation of digital filters to an upper frequency of one half of the sampling frequency. In the case of an optical comb-based RF photonic filter, this sampling rate corresponds to the comb repetition rate Δf. Note that in a network analyser measurement, which is based on coherent mixing with a reference tone, only a signal with frequency equal to that transmitted from the network analyser is acquired; other output tones are not detected. Nevertheless, to avoid spurious output tones, the frequency span should be restricted to fall within a single 'Nyquist zone', where the various Nyquist zones run from $p\Delta f/2$ through $(p+1)\Delta f/2$, where p is a non-negative integer. For figures in which the filter response is plotted over a range exceeding $\Delta f/2$, the boundaries between Nyquist zones are depicted as dashed vertical lines, similar to ref. 14. The FSR of our filters may be adjusted though the choice of fibre dispersion. For the data of Figs 1 and 6, due to the length of the available fibre, the filter FSRs fall close to 10 GHz, which is the boundary between the second and third Nyquist zones. For the data of Fig. 4, for which additional fibre was available, the FSR is $\sim$7.9 GHz, which places a filter peak near the centre of the second Nyquist zone.

Experiments demonstrating rapid filter reconfiguration made use of a 24 Gsample/s RF arbitrary waveform generator to generate the multiple-frequency RF input signal and a 50 Gsample/s real-time oscilloscope to digitize the time-domain filter output. In time-domain experiments, sampling effects were directly observable in the recorded traces when the measurement band exceeded one Nyquist zone. For the rapid tuning data reported in Fig. 3, an analogue low-pass filter with 4 GHz bandwidth was used to reject signals from other Nyquist zones. The time–frequency distribution of the filtered signal, Fig. 3d, was highlighted by computing a spectrogram of the oscilloscope data using a sliding fast Fourier transform window of 20.4 ns duration, with contour lines drawn at 5 dB intervals down to 20 dB.

Dual-comb filter tuning experiments. Our filter tuning experiments made use of a pair of nominally identical comb generators designed for approximately Gaussian spectra. From equation (2), the filter response can be seen to be sensitive to the difference in the frequency-dependent optical phase of the combs. A minimum filter bandwidth was obtained if the combs were identical so that their spectral phases cancelled. Although simulations indicate that the filter shape is robust against minor differences in the drive conditions of the two comb generators, we nevertheless attempted to generate two combs as close to identical as possible. The modulation indices on the phase modulators were matched by monitoring and comparing the individual optical spectra, and the indices of individual intensity modulators were set by monitoring their outputs on an RF spectrum analyser as the bias conditions were changed. Next, the RF phase (delay) between modulators was set by observing the comb with both RF and optical spectrum analysers. By watching for certain key

signatures (for example, a minimized comb line or harmonic), it was possible to very accurately set the proper bias and delay conditions and make the two combs very similar in terms of amplitudes and phases.

In the filter tuning experiments, propagation in the dispersive fibre led to a constant delay, or latency, between the control signal sent to the filter and the filter response. This latency was measured by connecting a continuous 4 GHz RF tone to the input of the filter (that is, to the single-sideband modulator) and a low-frequency (10 kHz) square wave (~50 ps rise time, 1 V amplitude) to the control port of the filter (that is, to the RF phase shifter). This scheme switches the filter passband alternately to coincide with or to miss the 4 GHz input, leading to a strong contrast in the output, which was observed with a real-time oscilloscope synchronized to the low-frequency square wave. This measurement yielded a latency of 26.0 μs.

Comb generation by cascaded FWM. In the comb source of Fig. 5a, the two c.w. lasers are spaced 10 nm apart. We operated the RF oscillator at 10 GHz, for which the V_π was ~9 V for the intensity modulators (IMs) and ~3 V for the phase modulators (PMs). IM1 was biased at quadrature with the RF amplitude of $0.5V_\pi$ zero to peak. IM2 was biased at the maximum transmission point with the RF amplitude of V_π. The transmission function is $a_1 = 0.5[1 + \exp(-j0.5\pi)\exp(j0.5\pi\cos(\omega_{RF}t))]$ for IM1 and $a_2 = 0.5[1 + \exp(j\pi\cos(\omega_{RF}t))]$ for IM2. The phase modulation $\varphi(t)$ was from the single-phase modulator, driven at its maximum RF input power (30 dBm) to maximize the modulation index seen by the gated pulses after IM2. The SMF used to delay one frequency with respect to the other by half a modulation period was ~300 m long. This was followed by a 1.5 W optical amplifier and a 100 m length of HNLF, with near-zero dispersion and low dispersion slope, to create a cascade of FWM terms. By use of a bandpass filter, we selected the FWM term centred at 1,562 nm. More details on the broadband comb generation process using cascaded FWM between two phase-modulated c.w. lasers can be found in ref. 50.

Received 6 May 2011; accepted 13 December 2011; published online 5 February 2012

References

1. Jones, D. J. *et al.* Carrier-envelope phase control of femtosecond mode-locked lasers and direct optical frequency synthesis. *Science* **288,** 635–639 (2000).
2. Udem, T., Holzwarth, R. & Hänsch, T. W. Optical frequency metrology. *Nature* **416,** 233–237 (2002).
3. Ma, L. S. *et al.* Optical frequency synthesis and comparison with uncertainty at the 10^{-19} level. *Science* **303,** 1843–1845 (2004).
4. Ye, J. & Cundiff, S. T. *Femtosecond Optical Frequency Comb: Principle, Operation, and Applications* (Springer, 2005).
5. Newbury, N. R. Searching for applications with a fine-tooth comb. *Nature Photon.* **5,** 186–188 (2011).
6. Delfyett, P. J. *et al.* Optical frequency combs from semiconductor lasers and applications in ultrawideband signal processing and communications. *J. Lightwave Technol.* **24,** 2701–2719 (2006).
7. Ellis, A. D. & Gunning, F. C. G. Spectral density enhancement using coherent WDM. *IEEE Photon. Technol. Lett.* **17,** 504–506 (2005).
8. Yamazaki, E., Inuzuka, F., Yonenaga, K., Takada, A. & Koga, M. Compensation of interchannel crosstalk induced by optical fiber nonlinearity in carrier phase-locked WDM system. *IEEE Photon. Technol. Lett.* **19,** 9–11 (2007).
9. Jiang, Z., Huang, C.-B., Leaird, D. E. & Weiner, A. M. Optical arbitrary waveform processing of more than 100 spectral comb lines. *Nature Photon.* **1,** 463–467 (2007).
10. Fontaine, N. K. *et al.* Real-time full-field arbitrary optical waveform measurement. *Nature Photon.* **4,** 248–254 (2010).
11. Cundiff, S. T. & Weiner, A. M. Optical arbitrary waveform generation. *Nature Photon.* **4,** 760–766 (2010).
12. Fortier, T. M. *et al.* Generation of ultrastable microwaves via optical frequency division. *Nature Photon.* **5,** 425–429 (2011).
13. Huang, C. B., Leaird, D. E. & Weiner, A. M. Time-multiplexed photonically enabled radio-frequency arbitrary waveform generation with 100 ps transitions. *Opt. Lett.* **32,** 3242–3244 (2007).
14. Hamidi, E., Leaird, D. E. & Weiner, A. M. Tunable programmable microwave photonic filters based on an optical frequency comb. *IEEE Trans. Microwave Theory Tech.* **58,** 3269–3278 (2010).
15. Ohara, T. *et al.* Over-1000-channel ultradense WDM transmission with supercontinuum multicarrier source, *J. Lightwave Technol.* **24,** 2311–2317 (2006).
16. Wu, R., Supradeepa, V. R., Long, C. M., Leaird, D. E. & Weiner, A. M. Generation of very flat optical frequency combs from continuouswave lasers using cascaded intensity and phase modulators driven by tailored radio frequency waveforms. *Opt. Lett.* **35,** 3234–3236 (2010).
17. Seeds, A. J. & Williams, K. J. Microwave photonics. *J. Lightwave Technol.* **24,** 4628–4641 (2006).
18. Capmany, J. & Novak, D. Microwave photonics combines two worlds. *Nature Photon.* **1,** 319–330 (2007).
19. Yao, J. P. Microwave photonics. *J. Lightwave Technol.* **27,** 314–335 (2009).
20. Haykin, S. Cognitive radio: brain-empowered wireless communications. *IEEE J. Select. Areas Commun.* **23,** 201–220 (2005).
21. Akyildiz, I. F., Lee, W. Y., Vuran, M. C. & Mohanty, S. Next generation/dynamic spectrum access/cognitive radio wireless networks: a survey. *Comput. Networks* **50,** 2127–2159 (2006).
22. Minasian, R. A. Photonic signal processing of microwave signals. *IEEE Trans. Microwave Theory Tech.* **54,** 832–846 (2006).
23. Capmany, J., Ortega, B., Pastor, D. & Sales, S. Discrete-time optical processing of microwave signals. *J. Lightwave Technol.* **23,** 702–723 (2005).
24. Rebeiz, G. M. *RF MEMS: Theory, Design, and Technology* (John Wiley & Sons, 2003).
25. Park, S. J., Reines, I., Patel, C. & Rebeiz, G. M. High-*Q* RF-MEMS 4–6-GHz tunable evanescent-mode cavity filter. *IEEE Trans. Microwave Theory Tech.* **58,** 381–389 (2010).
26. Liu, X., Katehi, L. P. B., Chappell, W. J. & Peroulis, D. High-*Q* tunable microwave cavity resonators and filters using SOI-based RF MEMS tuners. *IEEE J. Microelectromesh. Syst.* **19,** 774–784 (2010).
27. Savchenkov, A. A. *et al.* RF photonic signal processing components: from high order tunable filters to high stability tunable oscillators. *Proceedings of the 2009 IEEE Radar Conference* **1,** 1–6 (2009).
28. Ilchenko, V. & Maleki, L. Tunable radio frequency and microwave photonic filters. US patent 7,813,651 B2 (2010).
29. Madsen, C. K. & Zhao, J. H. *Optical Filter Design and Analysis: A Signal Processing Approach* (Wiley, 1999).
30. Harris, F. J. On the use of windows for harmonic analysis with the discrete Fourier transform. *Proc. IEEE* **66,** 51–83 (1978).
31. Oppenheim, A. V. & Schafer, R. W. *Discrete-Time Signal Processing*, 3rd edn (Prentice-Hall, 2009).
32. Ortigosa-Blanch, A., Mora, J., Capmany, J., Ortega, B. & Pastor, D. Tunable radio-frequency photonic filter based on an actively mode-locked fiber laser. *Opt. Lett.* **31,** 709–711 (2006).
33. Mora, J., Ortigosa-Blanch, A., Pastor, D. & Capmany, J. Tunable microwave photonic filter free from baseband and carrier suppression effect not requiring single sideband modulation using a Mach–Zehnder configuration. *Opt. Express* **14,** 7960–7965 (2006).
34. Lee, J. H., Chang, Y. M., Han, Y. G., Lee, S. B. & Chung, H. Y. Fully reconfigurable photonic microwave transversal filter based on digital micromirror device and continuous-wave, incoherent supercontinuum source. *Appl. Opt.* **46,** 5158–5167 (2007).
35. Chan, E. H. W. & Minasian, R. A. Coherence-free high-resolution RF/microwave photonic bandpass filter with high skirt selectivity and high stopband attenuation. *J. Lightwave Tech.* **28,** 1646–1651 (2010).
36. Weiner, A. M. Femtosecond pulse shaping using spatial light modulators. *Rev. Sci. Instrum.* **71,** 1929–1960 (2000).
37. Azaña, J., Berger, N. K., Levit, B. & Fischer, B. Spectro-temporal imaging of optical pulses with a single time lens. *IEEE Photon. Technol. Lett.* **16,** 882–884 (2004).
38. Torres-Company, V., Lancis, J. & Andrés, P. Lossless equalization of frequency combs. *Opt. Lett.* **33,** 1822–1824 (2008).
39. Sagues, M., Loayssa, A. & Capmany, J. Multitap complex-coefficient incoherent microwave photonic filters based on stimulated Brillouin scattering. *IEEE Photon. Technol. Lett.* **19,** 1194–1196 (2007).
40. Yan, Y. & Yao, J. A tunable photonic microwave filter with a complex coefficient using an optical RF phase shifter. *IEEE Photon. Technol. Lett.* **19,** 1472–1474 (2007).
41. Devgan, P. *et al.* Highly efficient multichannel wavelength conversion of DPSK signals. *J. Lightwave Technol.* **24,** 3677–3682 (2006).
42. Bres, C. S., Alic, N., Myslivets, E. & Radic, S. Scalable multicasting in one-pump parametric amplifier. *J. Lightwave Technol.* **27,** 356–363 (2009).
43. Ackerman, E. I. *et al.* Signal-to-noise performance of two analog photonic links using different noise reduction techniques. *Proceedings of the International Microwave Symposium* 51–54 (2007).
44. McKinney, J. D. *et al.* Sub-10-dB noise figure in a multiple-GHz analog optical link. *IEEE Photon. Technol. Lett.* **19,** 465–467 (2007).
45. McKinney, J. D. & Williams, K. J. Sampled analog optical Links, *IEEE Trans. Microwave Theory Tech.* **57,** 2093–2099 (2009).
46. McKinney, J. D., Briguglio J. & Urick V. J. Optical comb sources for suppression of stimulated Brillouin scattering in long-haul analog photonic links. *Proceedings of CLEO CFH2*, Baltimore, MD (2011).
47. Ma, Y. *et al.* 1-Tb/s per channel coherent optical OFDM transmission with subwavelength bandwidth access. *Proceedings of the National Fiber Optic Engineers Conference PDPC1*, San Diego, CA (2009).
48. Heck, M. J. R. & Bowers, J. E., Integrated Fourier-domain mode-locked lasers: analysis of a novel coherent WDM comb laser. *Proceedings of OFC JThA31*, Los Angeles, CA (2011).
49. Smith, G. H., Novak, D. & Zaheer, A. Overcoming chromatic-dispersion effects in fiber-wireless systems incorporating external modulators. *IEEE Trans. Microwave Theory Tech.* **45,** 1410–1415 (1997).

50. Supradeepa, V. R. & Weiner, A. M. A broadband, spectrally flat, high rep-rate frequency comb: bandwidth scaling and flatness enhancement of phase modulated CW through cascaded four-wave mixing. Preprint at http://arXiv:1010.2527 (2010).

Acknowledgements

This project was supported in part by the Naval Postgraduate School (grant no. N00244-09-1-0068) under the National Security Science and Engineering Faculty Fellowship programme. Any opinion, findings and conclusions or recommendations expressed in this publication are those of the authors and do not necessarily reflect the views of the sponsors. The authors thank V. Torres-Company, J. McKinney and D. Peroulis for helpful discussions.

Author contributions

C.M.L., R.W. and F.F. performed rapid tuning experiments, with assistance from E.H. V.R.S. and R.W. performed cascaded four-wave mixing experiments. R.W. performed bandwidth reconfiguration experiments with assistance from D.E.L. The project was organized and coordinated by A.M.W. A.M.W. led the writing of the manuscript, with contributions from V.R.S., C.M.L., R.W. and D.E.L.

Additional information

The authors declare no competing financial interests. Supplementary information accompanies this paper at www.nature.com/naturephotonics. Reprints and permission information is available online at http://www.nature.com/reprints. Correspondence and requests for materials should be addressed to A.M.W.